Annual and seasonal variabilities in the performances of wave energy converters

Nicolas Guillou, Georges Chapalain

Annual and seasonal variabilities in the performances of wave energy converters

Nicolas Guillou[a,*], Georges Chapalain[a]

[a] *Cerema, Direction Eau Mer et Fleuves, Environnement et Risques, Laboratoire de Génie Côtier et Environnement (LGCE), 155 rue Pierre Bouguer, Technopôle Brest-Iroise, BP 5, 29280, Plouzané, France*

Abstract

Locations of wave energy converters (WECs) are, most of the time, determined in areas with the highest density of mean wave power while ignoring the temporal variabilities of the resource. The most energetic regions are, however, characterised by strong inter- and intra-annual variations of wave power that may impact the energy production and performances of devices. We investigated these influences by focusing on the generated power from three well-known WECs that reached the stage of full-stage testing: Pelamis, AquaBuOY and Wave Dragon. This evaluation was conducted in western Brittany, one of the most energetic area along the coast of France. In comparison with the available resource, the generated technical power was characterised by reduced annual and seasonal variations. These effects were particularly noticeable for Pelamis that exhibited a reduced intermittency in the energy output between the winter and summer periods. The most energetic conditions had furthermore a restricted contribution to devices power output, mainly related to events with energy periods between 10.5 and 12.5 s, and significant wave heights between 2.75 and 4.25 m. WECs performances exhibited finally strong variabilities, in winter, with monthly-averaged values of the capacity factor up to 65% for Wave Dragon.

Keywords: Wave power matrix, Capacity factor, SWAN, Pelamis, AquaBuOY, Wave Dragon

1. Introduction

Among the different marine renewable energies (wind, tide, biomass, ocean thermal sources, osmotic...), the power of wind-generated surface-gravity waves presents an abundant resource, estimated at around 2 TW at the worldwide scale [1]. As wave energy may be characterised by a high power density in coastal waters [2], its exploitation has sparked, over the last decade, the most diverse technological developments with a wide range of wave energy converters (WECs) deployed in real sea conditions [3, 4]. In order to guarantee successful deployment of these devices and reduce the risk of investors,

*Corresponding author
Email address: nicolas.guillou@cerema.fr (Nicolas Guillou)

it is, however, essential to optimise their design and locations. Numerous studies were conducted to assess WECs performances in most promising locations for wave energy exploitation. A part of these investigations relied on wave buoy records as a refined reference to capture, at high temporal resolution, the variations of sea states distribution [5, 6, 7, 8]. These measurements are, however, not always available at locations of interest or cover (when recently implemented) a restricted period of time that can not encompass the inter- and intra-annual evolutions of the wave climate. Numerical modelling tools were thus, most of the time, retained to complement in-situ observations, and assess the technical power generated from a series of WECs (Tab. 1). These investigations were primarily targeted to the regions with the highest wave power including the west coast of Canada, the south-eastern part of Australia and the Atlantic European seafronts of Ireland, the United-Kingdom, France, Portugal and Spain [9].

Apart from a few exceptions [10, 19, 25, 27], most of these studies compared the averaged technical resource generated by a series of WECs in potential farm locations while ignoring the inter- and intra-annual variabilities of energy production. These aspects are, however, fundamental to consider as a device may show yearly-averaged high efficiency whereas the technology is designed for winter conditions, only. The generated energy may furthermore double from one year to another as a consequence of the inter-annual variability of the available wave power [19]. The energy output may finally show seasonal intermittency that requires refined investigations to guarantee balanced power output between offshore and nearshore locations, or along the coastline.

The present investigation complements the numerical evaluations of WECs performances in offshore and intermediate waters depths by exhibiting the inter- and intra-annual variabilities in the energy produced by a series of devices in real sea conditions. Following previous studies primarily targeted to regions with the highest density of wave power (Tab. 1), the site of application, here retained, is the western extend of Brittany

Table 1: Non-exhaustive review of regional and local evaluations in WECs performances based on high-resolution numerical wave power assessments. Three WECs are listed (Pelamis, AquaBuOY, and Wave Dragon) whereas these evaluations may consider other devices technologies such as [10] or [11] that rely on specific power matrices.

Study areas	Resource assessments		Selected WECs technologies			References
	Periods	Spatial resolutions	Pelamis	AquaBuoy	Wave Dragon	
Australia	31 years	up to 500 m	•	•	•	[12]
-	10 years	5 km	•	•	•	[13]
Canada	10 years	up to 50 m				[10]
China (south)	31 years	0.15^{o}	•	•	•	[14]
Denmark	3 months	50-100 m	•		•	[15]
Europe	11 years	0.75^{o}	•	•	•	[16]
-	3 years	880 m	•	•	•	[17]
-	10 years	0.75^{o}	•	•	•	[18]
France	58 years	0.25^{o}	•		•	[19]
Greece	35 years	0.025^{o}	•	•	•	[20, 21]
Ireland	5 years	200-500 m	•	•	•	[22]
Italy	5 years	200-500 m	•	•	•	[22]
Portugal	3 years	880 m	•	•	•	[23]
-	15 years	0.5^{o}	•		•	[24]
Spain	19 years	200 m	•	•		[25]
-	17 years	200 m	•			[26]
-	33 years	0.5'			•	[27]
United-Kingdom	11 years	0.025^{o}	•			[28]
-	10 years	1 km				[11]

(France, Fig. 1, Section 2.1), which is one of the most wave energetic region along the coast of France with averaged annual wave power estimated around 40 $\mathrm{kW\,m^{-1}}$ in offshore waters [29, 30]. This evaluation referred to three well-known WECs technologies that were widely considered in the numerical assessments of devices performances and reached the stage of full-scale testing in the marine environment (Tab. 1): Pelamis [31], AquaBuOY [32], and Wave Dragon [33]. The generated technical power was computed by combining wave scatter diagrams and WECs power matrices that provided, among wave heights and periods, the bivariate distribution of the sea states occurrence and the energy produced by devices, respectively. Wave scatter diagrams were obtained from a numerical evaluation of the wave energy resource, for a eight-year period (between 2004 and 2011) at high-spatial resolutions (up to 300 m in nearshore areas) [29] (Section 2.2). Devices power matrices derived from the publicly available technical data of the three technologies considered (Section 2.3). After an identification of most promising locations for WECs implementation in western Brittany (Section 3.1), the inter- and intra-annual variabilities of the generated technical resource and devices performances were successively analysed and compared, by exhibiting the temporal variations of WECs capacity factors and wave scatter diagrams (Sections 3.2, 3.3 and 3.4).

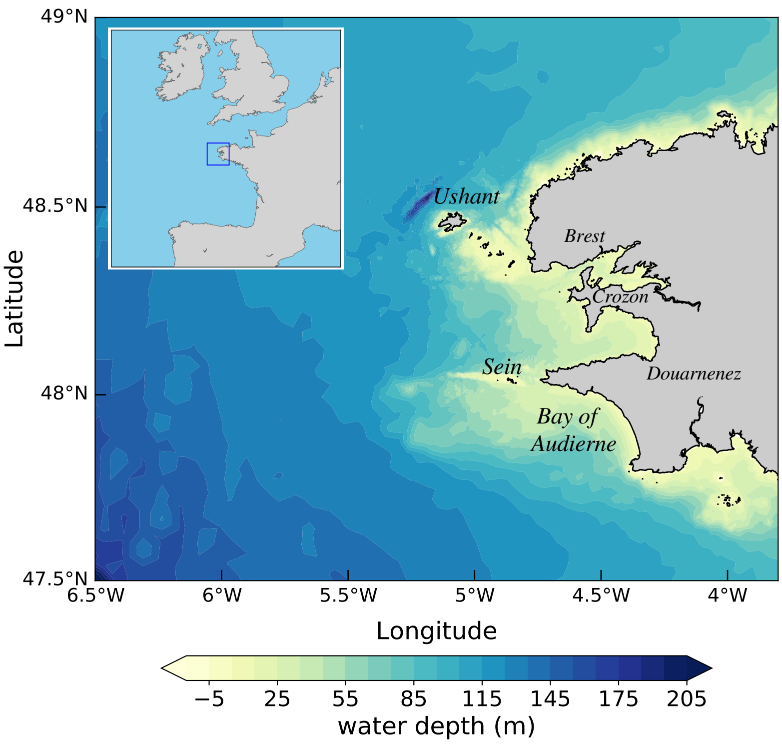

Figure 1: Bathymetry of western Brittany. Water depth is relative to mean sea level.

2. Materials and methods

2.1. *Study area*

The western extend of Brittany is a coastal environment, in north-western Europe, that borders the Celtic Sea and the Bay of Biscay with mean offshore water depths between 25 and 100 m (Fig. 1). The coastline consists in a variety of headlands and coastal basins characterised by the two prominent bays of Brest and Douarnenez. This environment is furthermore impacted by (i) strong wave regimes with offshore significant wave heights liable to exceed 10 m in storm winter conditions (Fig. 2-a) [29, 30], and (ii) tidal currents of more than 3.5 $m\,s^{-1}$ in mean spring conditions (Fig. 2-b) [34, 35, 36]. This area experiences thus strong interactions between waves and tidal currents [37, 38]. Tidal currents may lead to significant waves refraction and modulation of the incoming direction, resulting in semi-diurnal variations of the significant wave height by nearly 30% in deep waters [39]. Whereas numerous high-resolution numerical assessments of the wave energy resource were conducted along the Atlantic coast of France [29, 30, 40, 41, 42], no investigation focused on WECs performances in western Brittany. These evaluations appear, however, fundamental to promote the development of marine renewable energies within a french region that produces only 10% of its electricity consumption [43].

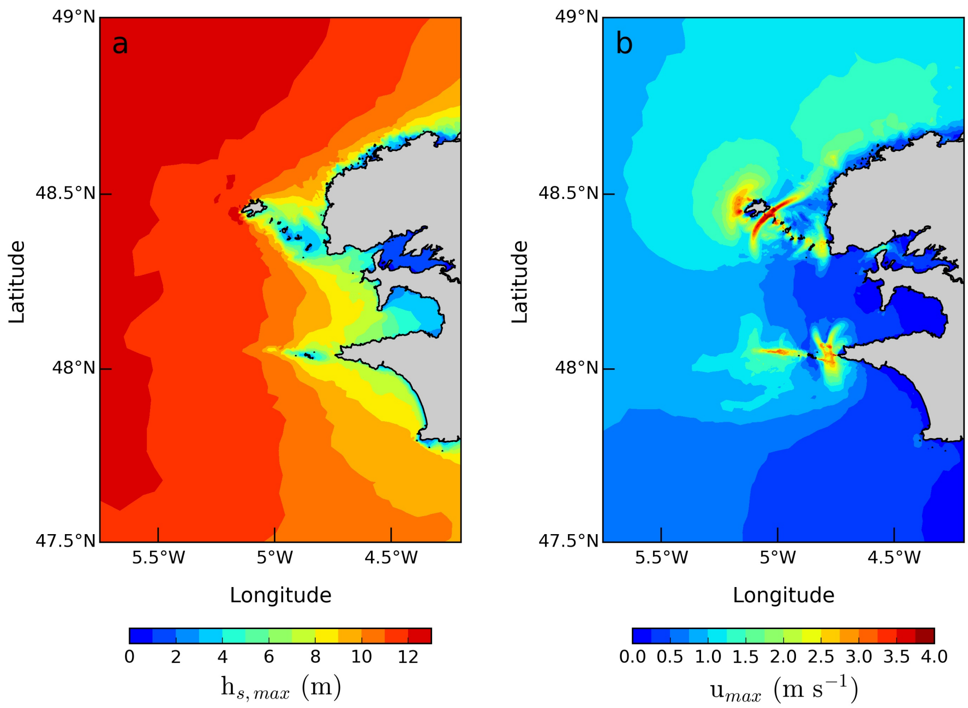

Figure 2: Predicted maximum (a) significant wave height over the period 2004-2011 [after 29] and (b) amplitude of depth-averaged tidal currents over a mean spring tidal cycle [after 35] in western Brittany.

2.2. Wave resource assessment

The spatio-temporal evolution of wave power was computed with the phase-averaged wave model SWAN [Simulating WAves Nearshore, 44] set up by Guillou and Chapalain [29], over the period between 2004 and 2011, in western Brittany. The model was implemented on an unstructured computational mesh with a nearshore spatial resolution of 300 m (Fig. 3). This resolution is a bit coarser than the value of 200 m recommended by Davey et al. [45] for numerical wave resource assessment. However, this refined spatial resolution was found to be mainly justified in areas with significant spatial variations of the bathymetry such as off the northern coast of Spain and the coast of Portugal characterised, offshore, by reduced footprint of the continental shelf [26, 46, 47, 48]. In comparison with these environments, the area of interest is characterised by reduced spatial variations of the bathymetry. In order to conduct long-term simulations at reduced computational cost, a spatial resolution of 300 m in the nearshore region was thus retained. The appropriateness of this resolution was confirmed with a comparison of wave predictions with measurements in nearshore waters [29]. This evaluation was consistent with the numerical sensitivity study conducted by Arean et al. [26] that exhibited slight differences in spectral wave predictions between spatial resolutions of 250 and 350 m. The wave model adopted furthermore a discretisation of 31 exponentially spaced frequencies ranging from 0.05 to 1 Hz, 30 evenly spaced directions and a time step of 15 min.

The dissipation of wave energy by bottom friction was evaluated in relation to the seabed roughness magnitude parametrised according to the heterogeneous distribution

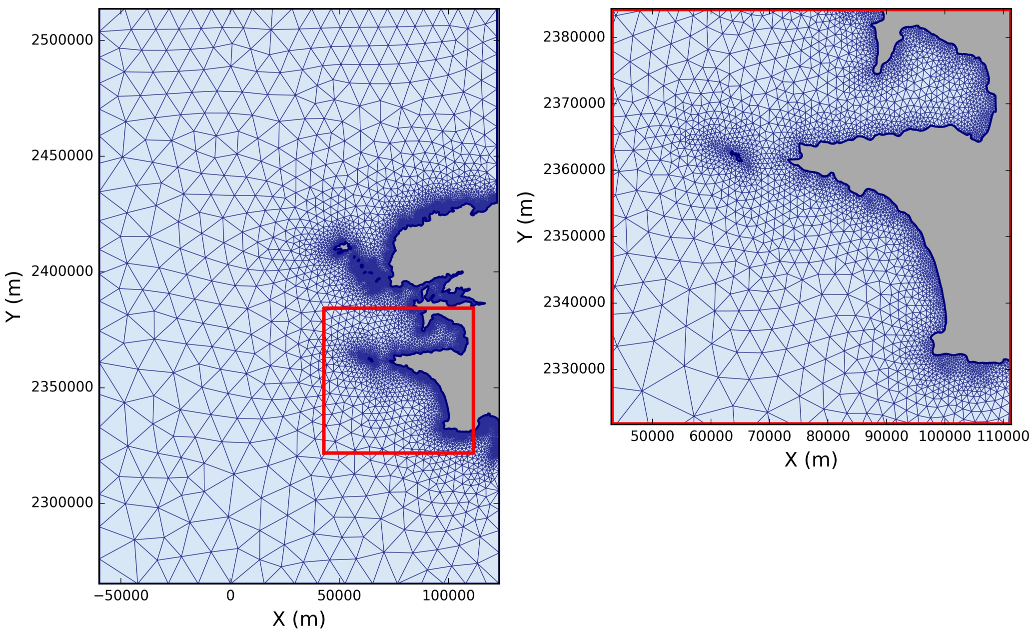

Figure 3: Overview of the unstructured computational grid for the wave propagation model with a detailed view in the south-western part of western Brittany where WECs implementation is considered (Section 3.1). Coordinates are indicated in metres according to the French system "Lambert II étendu".

of bottom sediments in the nearshore areas. Numerical simulations incorporated wind velocity components provided by the meteorological model ALADIN ("Aire Limitée, Adaptation dynamique, Développement InterNational, Météo-France) [49]. The wave spectral model integrated furthermore the variations of tidal free-surface elevation and depth-averaged currents predicted by the bidimensional horizontal circulation model TELEMAC 2D[50] set up at an extended computational grid. SWAN was finally driven by wave components (significant wave height, peak period, direction and spreading) extracted from regional Wavewatch III simulations conducted at the scale of the north-eastern Atlantic ocean in the context of the IOWAGA (Integrated Ocean WAves for Geophysical and other Applications) project [51].

Models predictions were finally evaluated against available measurements of the significant wave height H_s and the peak period T_p at nine locations in offshore and nearshore waters of western Brittany. Further details about model's parameterisation, setup and validation are available in Guillou and Chapalain [29]. The present investigation exploited the predicted distributions of sea states occurrence over H_s and T_p, and the available wave energy flux per unit crest length P_{wave}, with a time step of three hours at every computational grid nodes.

2.3. WEC technologies

The study considered technologies designed for offshore and intermediate mean water depths, over 25 m, setting aside devices for nearshore areas. Following most evaluations of devices performances (Tab. 1), we selected three WECs technologies: (i) Pelamis [31], (ii) AquaBuOY [32], and (iii) Wave Dragon [33].

Pelamis is an offshore, floating, slack-moored machine that is composed of four semi-submerged cylinders linked by hinged joints and oriented to the wave propagation direction. As waves pass along the length of the device, the different sections of the WEC bend and move relative to one another inducing a mechanical energy that is converted into electricity with power take-off control systems inside the joints. The Pelamis prototype, with a rated power of 750 kW, was selected for the investigation (Fig. 4).

AquaBuoy consists of a floater connected to a large cylinder, opened at both end below the sea surface [52]. This component, denominated as the accelerator tube, integrates a piston in its center and is connected to the top and bottom vertical extremities with a hose pump. As the buoy oscillates, the hose pump is stretched and compressed, thus discharging a flow of pressurised water to a Pelton turbine that is connected to a electricity generator. The device has a rated power of 250 kW (Fig. 5).

Wave Dragon is a floating, slack-moored device based on the principle of overtopping. The machine consists of two symmetrical reflecting wings that focus the waves towards a ramp. Behind, the overtopping water is collected and driven to a series of Kaplan turbines thus converting the difference of potential energy into electricity. The latest WEC concept, with a rated power of 5.9 MW, was retained here (Fig. 6).

2.4. Electricity production

The energy output of a WEC system (expressed in W.h), in a period of time ΔT, is computed as

$$E_{prod} = \sum_{i=1}^{nper} \sum_{j=1}^{nhs} f_{ij} p_{ij} \Delta T \tag{1}$$

Pelamis (kW)

H_s (m) \ T_e (s)	5	6	7	8	9	10	11	12	13
10.0									750
9.5								750	750
9.0							750	750	750
8.5						750	750	750	750
8.0					750	750	750	750	625
7.5				750	750	750	750	686	593
7.0				750	750	750	750	613	525
6.5			750	750	750	750	658	579	481
6.0			750	750	750	711	619	512	415
5.5			750	750	737	658	530	446	355
5.0			726	707	670	557	472	369	328
4.5		544	642	628	562	473	382	338	266
4.0		462	540	530	475	384	339	267	213
3.5		354	438	424	377	326	260	215	180
3.0	129	260	332	332	292	240	210	167	132
2.5	89	180	231	238	216	181	146	116	92
2.0	57	115	148	152	138	116	93	74	59
1.5	32	65	83	86	78	65	53	42	33
1.0		29	37	38	35	29	23		

Figure 4: Power matrix of Pelamis [from 7, 25, 53].

AquaBuOY (kW)

H_s (m) \ T_p (s)	6	7	8	9	10	11	12	13	14	15	16	17
5.5			250	250	250	250	250	211	172	172	172	92
5.0			250	250	250	250	214	175	142	142	142	77
4.5			223	250	239	208	173	142	115	115	115	62
4.0			122	176	198	188	164	137	112	91	91	49
3.5		93	135	152	144	126	105	86	70	70	70	38
3.0	54	68	99	111	106	92	77	63	51	51	51	27
2.5	37	47	69	77	73	64	54	43	36	36	36	19
2.0	24	30	44	49	47	41	34	28	23	23	23	12
1.5	13	17	25	27	26	23	19	15	12	12	12	7
1.0		8	11	12	11	10	8	7				

Figure 5: Power matrix of AquaBuOY [from 7].

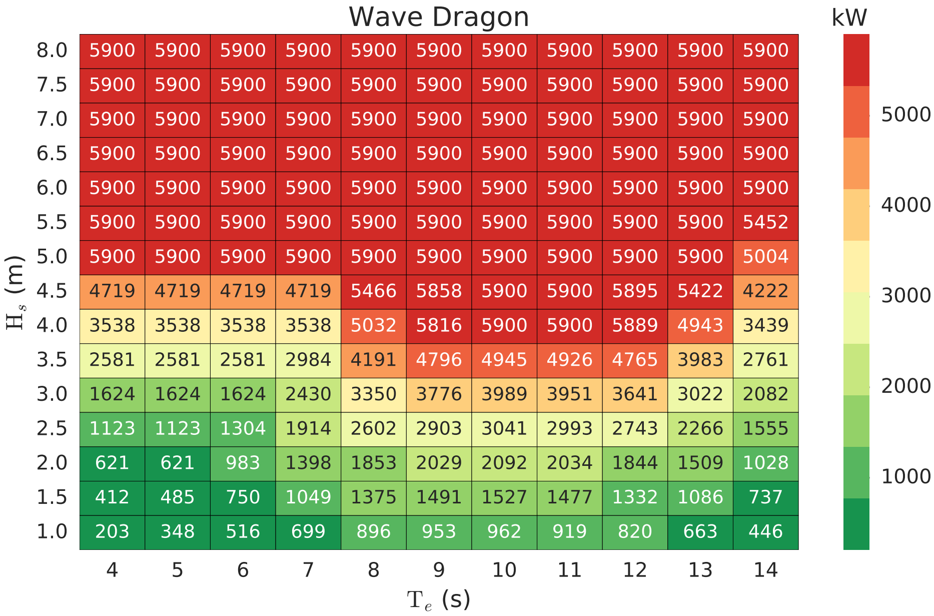

Figure 6: Power matrix of Wave Dragon [from 25].

where f_{ij} is the wave energy percentage occurrence and p_{ij} is the power generated by WEC for the i^{th} period class and the j^{th} wave height class. f_{ij} derives from the wave scatter diagram computed over the time period ΔT at the selected location while p_{ij} is reported by the power matrix of the WEC considered (Figs. 4-6). *nper* and *nhs* are the numbers of period and wave height classes considered, respectively. As numerical simulations did not output the wave energy period T_e commonly provided by WECs developers, its value was estimated based on the peak period T_p as $T_e = \alpha T_p$ with α a coefficient that depends on the wave spectrum shape. Following [19, 54, 55], its value was taken equal to $\alpha = 0.9$. This corresponds to a standard JONSWAP spectrum with a peak enhancement $\gamma = 3.3$. Some uncertainty may thus exist in the approach of the generated wave power. It was estimated, however, that offshore, errors in period were less important than errors in wave height as the wave power density is proportional to $T_e H_s^2$ [55]. Power matrices may finally adopt different discretisations among wave heights and periods. In order to reduce the sensitivity of these evaluations to the discretisations of power matrices, the investigation adopted constant intervals of (i) 1 s for wave periods and (ii) 0.5 m for significant wave heights.

The performance of WECs was finally evaluated with the capacity factor

$$C_f = 100 \frac{P_{prod}}{P_{rated}} \tag{2}$$

defined as the ratio between the averaged power produced by a device $P_{prod} = E_{prod}/\Delta T$ and its rated power P_{rated}. This parameter accounts thus for the fraction of the time the energy converter is operating at full capacity. The temporal variabilities of the available wave energy flux, the generated wave power, and the devices capacity factors were finally evaluated with a series of parameters including the minimum and maximum values, and the standard deviation

$$STD = \sqrt{\frac{1}{n}\sum_{i=1}^{n}(x_i - \bar{x})^2} \quad (3)$$

where n is the number of data in the discretised series considered, (x_i) represents the simulated values, and $\bar{x}$ its mean value.

3. Results and discussion

3.1. Potential locations

Neglecting further considerations associated with the practical, political, environmental issues and marines activities, the implementation of WECs has to satisfy physical constrains based on the mean water depths and the hydrodynamic conditions. Pelamis and AquaBuOY are thus designed for offshore locations, in water depths between 50 and 70 m [8, 23, 56], whereas Wave Dragon is planned to operate in intermediate waters, usually between 25 and 40 m [22, 23]. In order to guarantee secure moorings of devices, currents must furthermore have moderate amplitudes, estimated below 0.5 $m\,s^{-1}$ for Pelamis [56]. In western Brittany, the attention was thus dedicated to areas with mean water depths between 25 and 70 m, and peak tidal currents below 0.5 $m\,s^{-1}$ in mean spring conditions, for the three WECs technologies selected. Two databases were considered to apply these criteria. The spatial distribution of the mean water depth derived from the HOMONIM database ("Historique, Observation, MOdélisation des NIveaux Marins", SHOM, Météo-France) that covers the area of interest with a spatial resolution of 111 m [57]. The amplitude of mean spring tidal currents was obtained from predictions established by Guillou and Chapalain [35] relying on a high-resolution three-dimensional tidal circulation model in western Brittany.

Potential locations for WECs implementation were identified in restricted areas, off the Crozon Peninsula and in the bay of Audierne (Fig. 7). Considering marine waterways at the entrance of the bay of Brest and the bay of Douarnenez, a series of five locations was selected for the evaluation of WECs performances: (i) three locations in offshore waters (50-70 m, #1, #2 and #3) for Pelamis and AquaBuOY, and (ii) two locations in intermediate water depths (25-40 m, #4 and #5) for Wave Dragon (Fig. 7 and Tab. 2). No location was retained for Wave Dragon in the bay of Douarnenez that was characterised by weak energetic wave regime during the eight-year period simulated (between 2004 and 2011). These five potential locations exhibited furthermore a reduced variability in the directional distribution of wave power (Fig. 8). Numerical predictions were thus exploited disregarding the incoming wave direction that may influence the performances of WECs, in particular devices designed to capture wave energy in a given orientation.

A refined investigation was conducted to evaluate the parameter WEC_{op} defined as the percentage of time the device was operating over the period 2004-2011 (Table 2). This evaluation was performed by quantifying the number of waves events that produce energy in the three power matrices considered (Figs. 4-6). At the five locations retained, devices operated thus for more than 84% of the time over the period 2004-2011. Wave Dragon

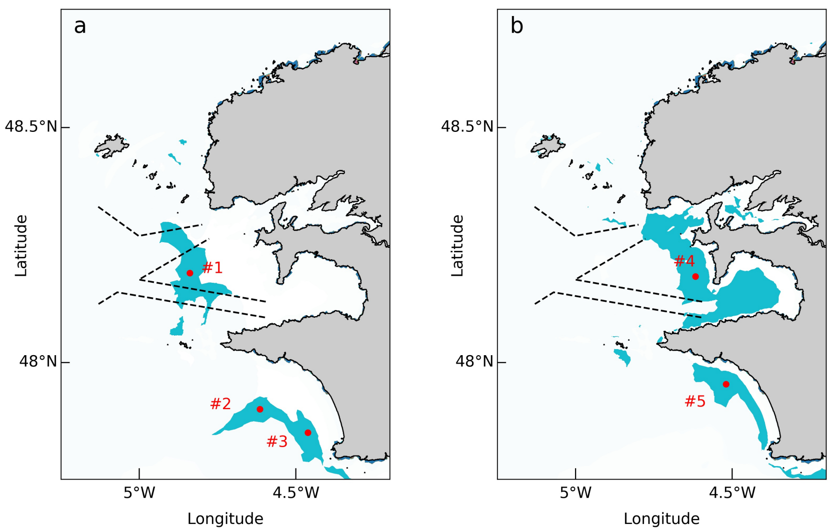

Figure 7: Areas (in light blue) with mean water depths between (a) 50 and 70 m and (b) 25 and 40 m, and mean spring tidal currents below 0.5 $m\,s^{-1}$. Red circles show the locations #1 to #5 considered for the evaluation of WECs performances. The dotted black lines show the ship routes at the entrance of the bay of Brest and the bay of Douarnenez.

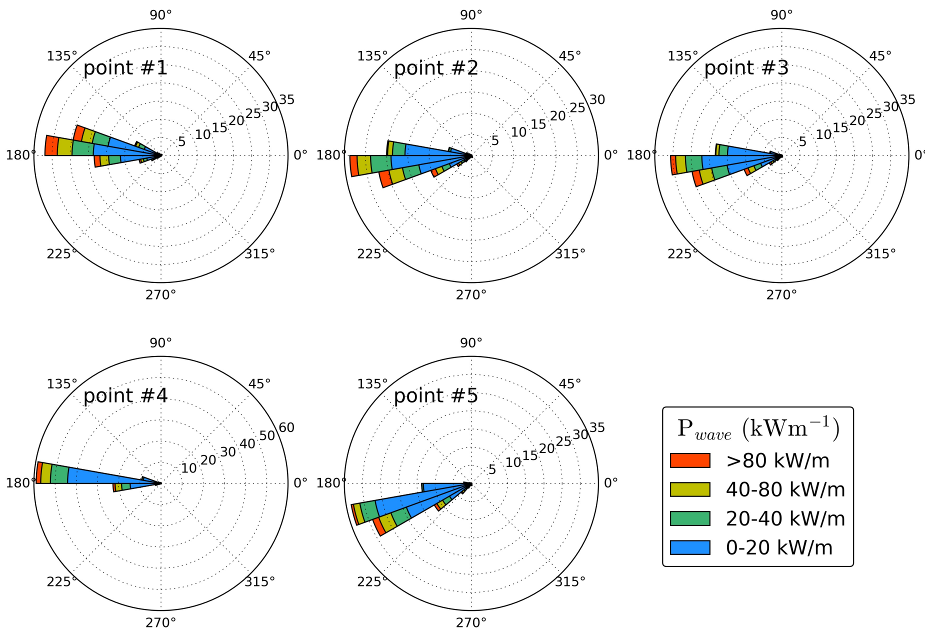

Figure 8: Predicted directional distribution of the available wave energy flux per unit crest length at points #1 to #5 over the period 2004-2011.

produced naturally the greatest energy in relation to its power rated at 5.9 MW (Tab. 3). The averaged energy generated by a single Wave Dragon device during a year was thus estimated at around 13 GW.h at both locations in intermediate water depths (#4 and #5). This corresponds to the electricity demand of around 2117 houses, by considering an annual consumption of 6.14 MW.h during a year for a house in France [58]. The averaged capacity factor of Wave Dragon was furthermore estimated around 25% at points #4 and #5 while it remained below 18%, for Pelamis and AquaBuOY, at offshore locations #1, #2 and #3. Such discrepancy between Wave Dragon and Pelamis was reported by Sierra et al. [19] along the south-western Atlantic coast of France. This investigation, based on wave predictions over 58 years (1958-1999), provided averaged capacity factors between 23.9 and 27.9% for Wave Dragon while being restricted below 16.3% for Pelamis. These averaged estimations of WECs performances depend, however, strongly on the adaptation of devices to the wave conditions at a given location. In offshore waters of northern Galicia (Spain), Carballo et al. [25] exhibited thus stronger performances of Pelamis and AquaBuOY. Their 19-year (1996-2014) numerical evaluation of wave conditions reported averaged capacity factors of 27.0% for Pelamis and 26.3% for AquaBuOY. A part of these differences may furthermore be imputed to the temporal variability of the wave climate liable to influence the quantification of the mean wave power and energy output over different periods of time. In western Brittany, the offshore mean wave energy flux was thus estimated at 40 kWm^{-1} by relying on a 8-year (2004-2011) numerical assessment [29] whereas it was computed at 50 kWm^{-1} by exploiting predictions over a 23-year (1979-2001) period [59]. A refined comparison of WECs performances can not be well established on temporal averaged parameters, and it is essential to gain further insights about the annual and seasonal variabilities of the generated power (Sections 3.2 and 3.3).

Table 2: Locations considered for the evaluation of WECs performances with (i) mean water depths and (ii) WEC$_{op}$ that corresponds to the percentage of time the device is operating and produces energy over the period 2004-2011.

Location number	Coordinates Lon.	Coordinates Lat.	Mean water depth (m)	WEC$_{op}$ Pelamis	WEC$_{op}$ AquaBuOY	WEC$_{op}$ Wave Dragon
#1	4.84°W	48.19°N	61.5	88.6%	91.3%	
#2	4.61°W	47.90°N	62.2	88.3%	91.4%	
#3	4.46°W	47.85°N	56.7	86.6%	90.2%	
#4	4.62°W	48.18°N	36.4			85.4%
#5	4.52°W	47.95°N	35.7			84.5%

Table 3: Mean available wave energy flux P_{mean}, mean energy produced by WECs during a year E_{mean}, and mean capacity factor C_f at locations #1 to #5 over the period 2004-2011.

Location number	P_{mean} (kWm^{-1})	Pelamis E_{mean} (GW.h)	Pelamis C_f	AquaBuOY E_{mean} (GW.h)	AquaBuOY C_f	Wave Dragon E_{mean} (GW.h)	Wave Dragon C_f
#1	28.1	1.03	15.7%	0.39	17.9%		
#2	23.8	0.91	13.9%	0.35	15.8%		
#3	21.8	0.83	12.6%	0.31	14.3%		
#4	18.4					13.1	25.3%
#5	17.5					12.8	24.8%

3.2. Yearly-averaged performances

As exhibited by Sierra et al. [19], the inter-annual evolution of the wave power, along the south-western Atlantic coast of France, may be characterised by strong variability with differences ratio of up to three between two different years. The medium-term evaluation, conducted in western Brittany, exhibited a part of this variability that may influence the performances of WECs. The annual variabilities of devices performances were thus evaluated by relying on yearly-averaged capacity factors of devices between 2004 and 2011 (Fig. 9). This investigation was restricted to the area off the Crozon Peninsula (points #1 and #4), as similar variations of WECs performances were obtained in the bay of Audierne (points #2, #3 and #5).

Over the area selected, the yearly-averaged performances of WECs (Fig. 9) corroborated differences on values of the capacity factor averaged over the period 2004-2011 (Section 3.1). Wave Dragon was thus characterised by the highest yearly-averaged capacity factors whereas the available wave energy flux at its location (#4) was significantly reduced in comparison with the offshore point (#4), in relation to the dissipation of wave energy by bottom friction in intermediate water depths [29, 60].

Except for years 2007 and 2008, the capacity factors of WECs followed furthermore the evolution of the available wave wave energy flux. Differences in devices capacity factors were, however, smoothed in comparison with the available wave energy flux. The

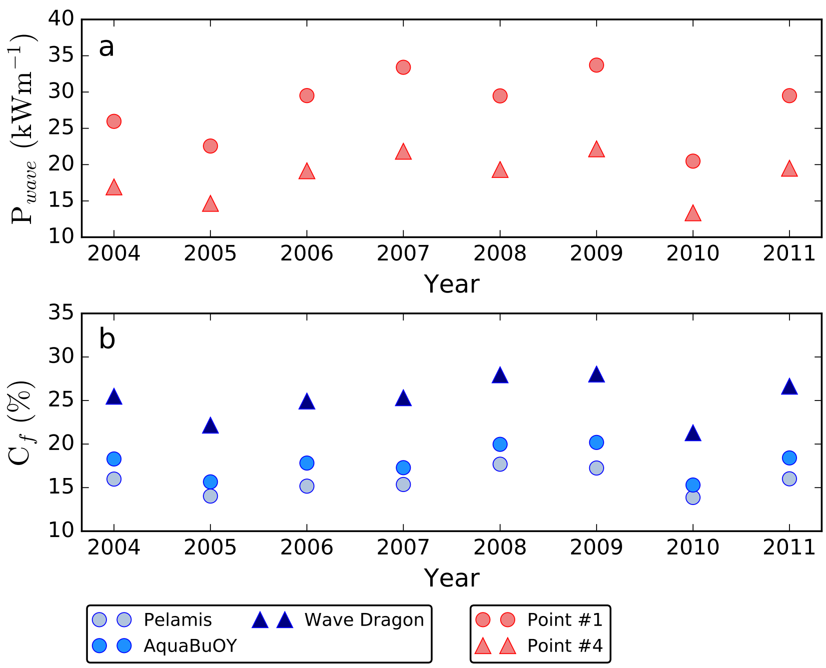

Figure 9: Yearly-averaged (a) available wave energy flux at points #1 and #4 and (b) capacity factors of WECs at points #1 (for Pelamis and AquaBuOY) and #4 (for Wave Dragon). Circles refer to point #1 while triangles refer to point #4.

averaged power produced by Wave Dragon was thus found to vary by 24% between the most (2009) and the less (2010) energetic years while the available wave energy flux exhibited a difference by nearly 40%. Further investigations were conducted, at monthly time scales, to exhibit the filter effects that the power matrices of WECs may have on the generated energy.

3.3. Monthly-averaged performances

As exhibited on yearly-averaged quantities (Section 3.2), monthly-averaged variations of the generated wave energy were characterised by smoothed evolutions in comparison with the available power (Figs. 10 and 11). This was reported on (i) the seasonal contrast between the winter and summer periods and (ii) the inter-annual variabilities of the winter energetic months. Indeed, the available wave energy flux was characterised by a clear contrast between (i) winter energetic conditions of December, January and February and (ii) summer conditions of June, July and August [19, 41, 61]. Off the Crozon Peninsula (point #1), the monthly-averaged wave energy flux was thus 6.6 times larger in January than in June (Fig. 10). However, smoothed variations of devices capacity factors were obtained between the winter and summer periods (Fig. 11). This was particularly noticeable for Pelamis whose averaged capacity factors varied between 18.8% in winter and 12.0% in summer at point #1 (Fig. 12-a). Besides these intra-annual variations, the available energy potential, off the Crozon Peninsula, exhibited significant inter-annual variabilities [29, 30]. While the available wave energy flux remained nearly stable between April and September, strong annual differences were obtained during autumn and winter, that presented the most energetic conditions. P_{wave} was thus multiplied by 1.9 between February 2010 and 2011, increasing from 44.7 $\mathrm{kW\,m^{-1}}$ to 84.1 $\mathrm{kW\,m^{-1}}$. However, disregarding the month of November that presented a high-power density in 2009, the productions of devices were characterised by reduced inter-annual variations. Over this period, the capacity factor of Pelamis reported thus standard deviations below 5.7% at point #1 (Fig. 11-a). In spite of reduced performances of devices, these smoothed seasonal and inter-annual variations may appear of interest to reduce the intermittency of the generated power at a given location.

A comparison of devices performances was finally conducted by relying on monthly-averaged values of the capacity factor. Although subjected to reduced energetic sea states in intermediate water depths (point #4, Sections 3.1 and 3.2), Wave Dragon exhibited the highest monthly-averaged capacity factor with values liable to reach 65% in November 2009 (Fig. 11-f). The averaged capacity factor of Wave Dragon was furthermore estimated at 33.1% in winter and 17.3% in summer. The areas located off the Crozon Peninsula were finally characterised by higher capacity factors for Pelamis and AquaBuOY than locations identified in the bay of Audierne (Figs. 12-a and -b). Whereas reduced differences were obtained, in intermediate water depths, for Wave Dragon, these results promote the areas identified off the Crozon Peninsula to develop and implement WECs in western Brittany. Wave Dragon appears thus as an attractive technology to conduct this development, as it exhibited (i) the highest capacity factors and rated powers, and (ii) a design adapted to intermediate water depths with restricted distance from shore and reduced costs associated with electrical cables.

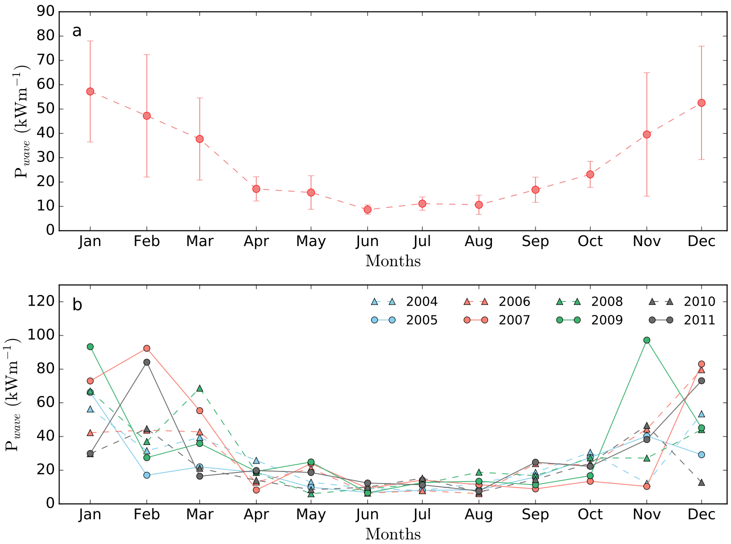

Figure 10: (a) Time series of the mean eight-year available wave energy flux with its standard deviation (in vertical lines) at point #1; and (b) yearly time series of the monthly averaged available wave energy flux over the period 2004-2011.

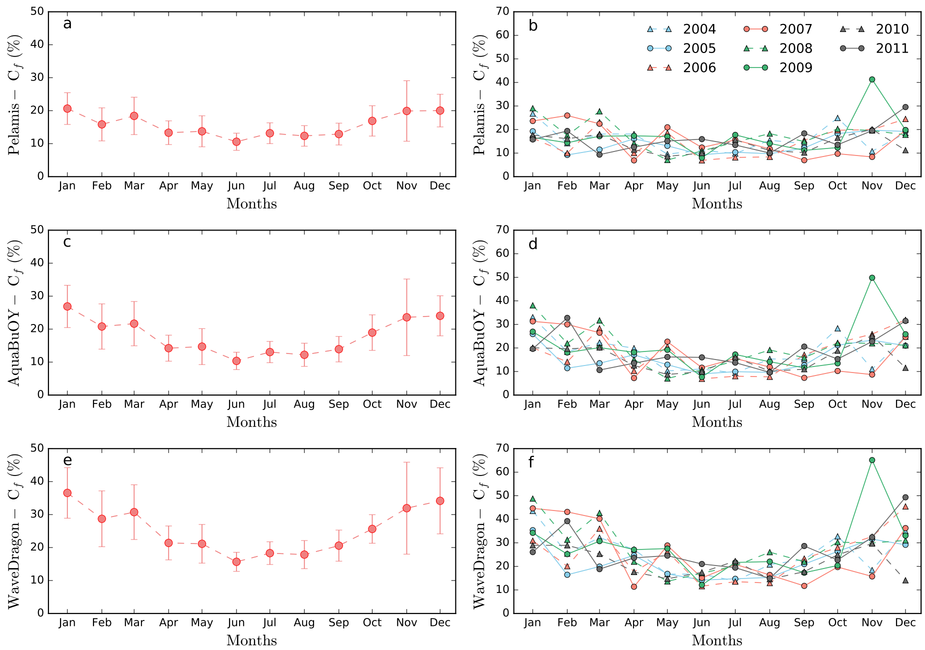

Figure 11: Time series of the overall generated wave power with its standard deviation for (a) Pelamis and (c) AquaBuOY at point #1; and (e) Wave Dragon at point #4; and (b, d, f) yearly associated time series over the period 2004-2011.

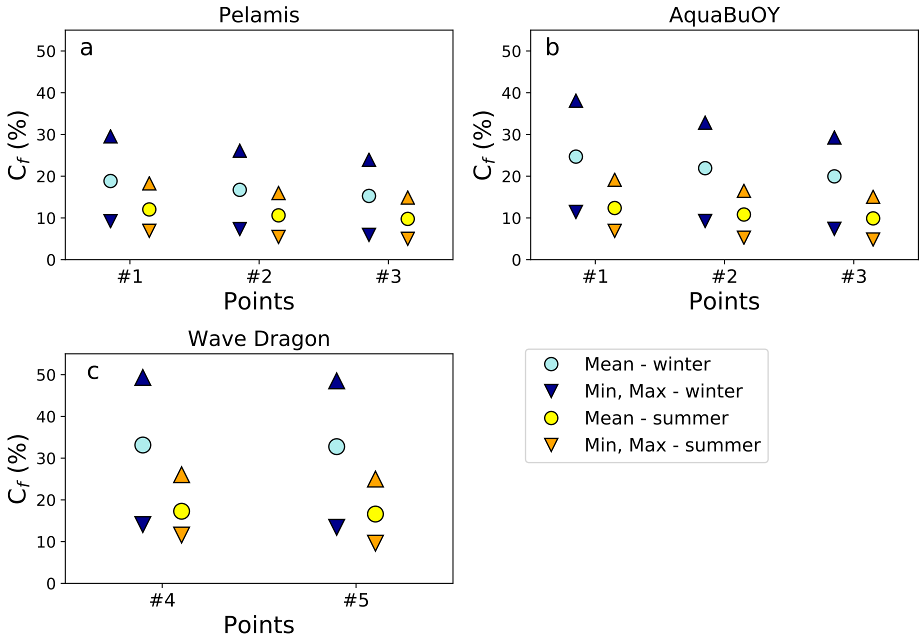

Figure 12: Averaged, maximum and minimum monthly-averaged capacity factors in winter (December-January-February) and summer (June-July-August) periods between 2004 and 2011 for Pelamis, AquaBuOY and Wave Dragon at locations #1 to #5.

3.4. Wave scatter diagrams and power matrices

In order to provide further insights about the annual and seasonal variabilities of the generated power, particular attention was finally dedicated to the evolution of wave scatter diagrams off the Crozon Peninsula, and their correlation with the power matrices of WECs. Highest values of devices generated power were naturally found in conditions of close correlation between wave scatter diagrams and devices power matrices. The averaged wave scatter diagram for the month of November 2009 exhibited such strong correlation, with waves events mainly distributed between (i) energy periods of 9.5 and 12.5 s and (ii) significant wave heights of 3.75 and 5.25 m (Fig. 13). This range of wave periods and heights was in/or at the limit of the maximum operational function of the three WECs considered (Figs. 4, 5 and 6). The highest contribution to power output in November 2009, obtained for waves events around T_e = 10 s and H_s = 4.0 m, reached thus the rated power of Wave Dragon (Figs. 6 and 13). This explains the highest capacity factor estimated for this device in November 2009. Whereas these waves events were not representative of the most energetic situations, they contributed to the significant part of energy generation. This confirms the investigations conduced by Sierra et al. [19] who exhibited the restricted effects of energetic sea states on power generation in the Bay of Biscay.

These waves events were, however, more prevalent in winter than in summer that was characterised by an increased distribution of energy periods between 6.5 and 9.5 s, and significant wave heights below 2.75 m (Fig. 14-a). This summer distribution,

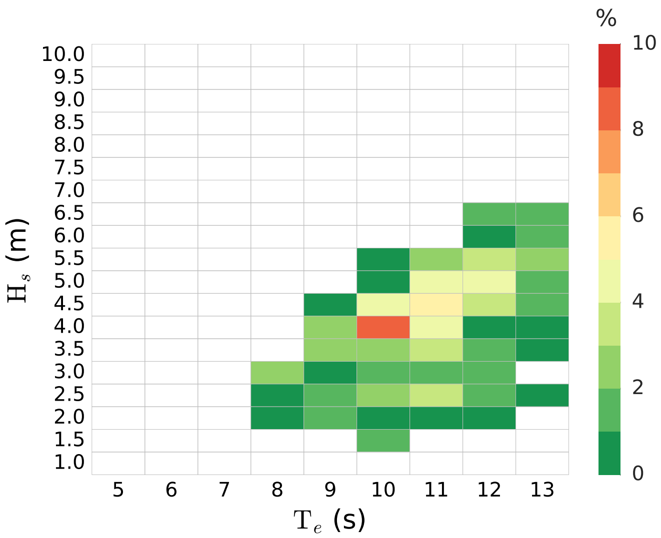

Figure 13: Mean distribution of waves events, over a range of H_s and T_e, in November 2009 at point #1.

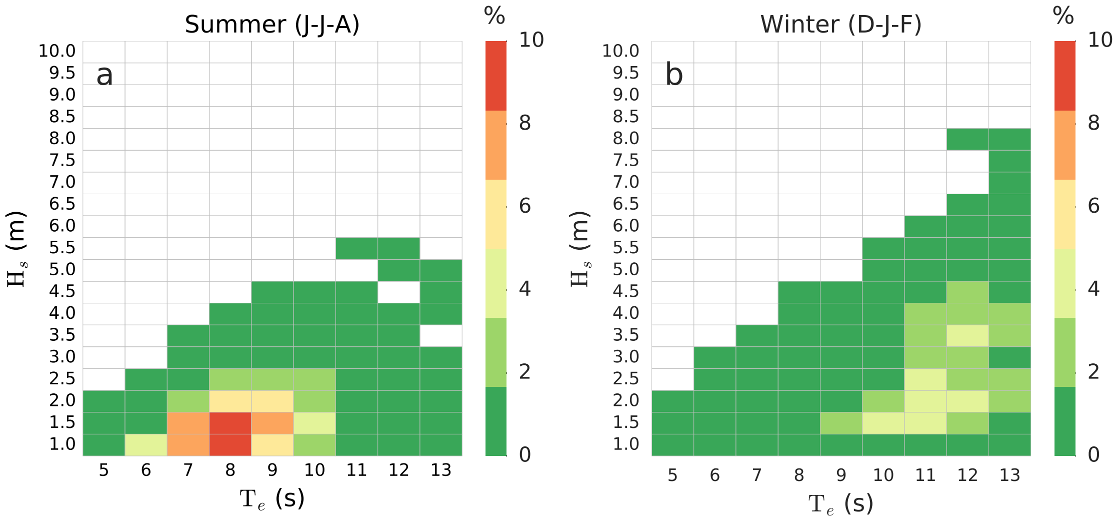

Figure 14: Mean distribution of waves events, over a range of H_s and T_e, in summer and winter at point #1.

that was clearly out of the range of maximum WECs efficiency, induced reduced performances of devices. Off the Crozon Peninsula, at point #1, the dominant proportion ($\simeq 21\%$) of summer waves events were thus obtained for T_e between 7.5 and 8.5 s, and H_s between 0.75 and 1.75 m (Fig. 14-a), which may generate a maximum power of 86 kW (C_f = 11.5%) and 25 kW (C_f = 10%) for Pelamis and AquaBuOY, respectively. These scatter diagrams provided finally an explanation about the attenuated variations of energy output at annual and seasonal scales. Indeed, in winter, waves events were mainly distributed between T_e of 10.5 and 12.5 s, and H_s of 2.75 and 4.25 m, and only a restricted part of the available wave energy flux contributed to power generation (Fig. 14-b).

4. Conclusions

Medium-term predictions of waves conditions (between 2004 and 2011) were exploited to assess the potential locations and the performances of a series of three WECs technologies (Pelamis, AquaBuOY and Wave Dragon) in western Brittany. Besides a simple comparison based on yearly-averaged values, this investigation exhibited the inter- and intra-annual variabilities of the generated powers and capacity factors of devices. The main outcomes of the present study are as follows:

1. Locations of interest for WECs implementation were identified, in offshore and intermediate waters depths, off the Crozon Peninsula and in the bay of Audierne. According to devices capacity factors, the area identified off the Crozon Peninsula appears the most promising for the preliminary development and implementation of WECs.
2. In comparison with the available wave energy flux that showed high annual and seasonal variations, the generated power of WECs were characterised by smoothed differences in relation to filter effects associated with devices power matrices. These effects were particularly noticeable for Pelamis with a reduced seasonal intermittency in the energy output between the winter and summer periods.
3. The variation of WECs generated powers depends on the correlation between wave scatter diagrams and devices power matrices. The most energetic wave conditions did not contribute significantly to power generation, that was mainly related, in offshore waters, to winter waves events with periods between 10.5 and 12.5 s and wave heights between 2.75 and 4.25 m.
4. While Wave Dragon was implemented in intermediate water depths, between 25 and 40 m, with significant attenuation of the available wave energy flux in comparison with offshore waters, this device provided the highest capacity factors with winter-averaged values estimated at around 33%. Monthly-averaged values were furthermore liable to exceed 65% in November 2009, which is a noticeable capacity factor for WECs.

This investigation provided further insights on WECs implementation in western Brittany exhibiting that high performances may be reached, especially during the winter period, in spite of reduced yearly-averaged values. The inter- and intra-annual variabilities of the generated power are thus to consider to guarantee successful design and deployment of devices in the marine environment. This medium-term evaluation of WECs performances will, however, benefit from long-term assessments of wave conditions exhibiting the variability of the available and generated resources over several decades. Indeed, the evolution in the probability of high energetic events, characterised by higher wave heights and periods, presents clear consequences for wave energy production. In the area of interest, high-resolution numerical modelling may finally be conducted to integrate the effects of wave energy extraction on the wave field and generated powers.

Acknowledgements

The present paper is a contribution to the research program DIADEME ("Design et InterActions des Dispositifs d'extraction d'Energies Marines avec l'Environnment") of the Laboratory of Coastal Engineering and Environment (LGCE, Cerema).

References

[1] K. Gunn, C. Stock-Williams, Quantifying the global wave power resource, Renewable Energy 44 (2012) 296–304.

[2] A. Clément, P. McCullen, A. Falcão, A. Fiorentino, F. Gardner, K. Hammarlund, G. Lemonis, T. Lewis, K. Nielsen, S. Petroncini, M. T. Pontes, P. Schild, B. O. Sjöström, H. C. Sørensen, T. Thorpe, Wave energy in Europe: current status and perspectives, Renewable & Sustainable Energy Reviews 6 (2002) 405–431.

[3] A. Falcão, Wave energy utilization: a review of the technologies, Renewable & Sustainable Energy Reviews 14 (2010) 899–918.

[4] S. Lindroth, M. Leijon, Offshore wave power measurements - A review, Renewable & Sustainable Energy Reviews 15 (2011) 4274–4285.

[5] M. O'Connor, T. Lewis, G. Dalton, Techno-economic performance of the Pelamis P1 and Wavestar at different ratings and various locations in Europe, Renewable Energy 50 (2013) 889–900.

[6] B. Cahill, T. Lewis, Wave energy resource characterisation of the Atlantic Marine Energy Test Site, International Journal of Marine Energy 1 (2013) 3–15.

[7] S. Diaconu, E. Rusu, Evaluation of various WEC devices in the Romanian near shore, in: Proceedings of Advances in Environment Technologies, Agriculture, Food and Animal Science, 2013.

[8] S. Bozzi, R. Archetti, G. Passoni, Wave electricity production in Italian offshore: A preliminary investigation, Renewable Energy 62 (2014) 407–416.

[9] L. Rusu, F. Onea, The performance of some state-of-the-art wave energy converters in locations with the worldwide highest wave power, Renewable & Sustainable Energy Reviews 75 (2017) 1348–1362.

[10] B. Robertson, C. Hiles, E. Luczko, B. Buckham, Quantifying wave power and wave energy converter array production potential, International Journal of Marine Energy 14 (2016) 143–160.

[11] I. Fairley, H. C. M. Smith, B. Robertson, M. Abusara, I. Masters, Spatio-temporal variation in wave power and implications for electricity supply, Renewable Energy 114 (2017) 154–165.

[12] J. Morim, N. Cartwright, A. Etemad-Shahidi, D. Strauss, M. Hemer, Wave energy resource assessment along the Southeast coast of Australia, Applied Energy 184 (2016) 276–297.

[13] S. Behrens, J. Hayward, M. Hemer, P. Osman, Assessing the wave energy converter potential for Australian coastal regions, Renewable Energy 43 (2012) 210–217.

[14] A. Mirzaei, F. Tangang, L. Juneng, Wave energy potential assessment in the central and southern regions of the South China Sea, Renewable Energy 80 (2015) 454–470.

[15] J. Fernández-Chozas, N. Helstrup Jensen, H. Sørensen, J. Kofoed, A. Kabuth, Predictability of the power output of three wave energy technologies in the Danish North Sea, International Journal of Marine Energy 1 (2013) 84–98.

[16] L. Rusu, F. Onea, Assessment of the performances of various wave energy converters along the European continental coasts, Energy 82 (2015) 889–904.

[17] E. Rusu, Evaluation of the Wave Energy Conversion Efficiency in Various Coastal Environments, Energies 7 (2014) 4002–4018.

[18] E. Rusu, F. Onea, Estimation of the wave energy conversion efficiency in the Atlantic Ocean close to the European islands, Renewable Energy 85 (2016) 687–703.

[19] J. Sierra, A. White, C. Mösso, M. Mestres, Assessment of the intra-annual and inter-annual variability of the wave energy resource in the Bay of Biscay (France), Energy 141 (2017) 853–868.

[20] G. Lavidas, V. Venugopal, A 35 year high-resolution wave atlas for nearshore energy production and economics at the Aegean Sea, Renewable Energy 103 (2017) 401–417.

[21] G. Lavidas, Energy and socio-economic benefits from the development of wave energy in Greece, Renewable Energy 132 (2019) 1290–1300.

[22] V. Vannuchi, L. Cappietti, Wave Energy Assessment and Performance Estimation of State of the Art Wave Energy Converters in Italian Hotspots, Sustainability 8 (1300).

[23] D. Silva, E. Rusu, C. Guedes Soares, Evaluation of various technologies for wave energy conversion in the Portuguese Nearshore, Energies 6 (2013) 1344–1364.

[24] P. Mota, J. Pinto, Wave energy potential along the western Portuguese coast, Renewable Energy 71 (2014) 8–17.

[25] R. Carballo, M. Sánchez, V. Ramos, J. Fraguela, G. Iglesias, The intra-annual variability in the performance of wave energy converters: A comparative study in N Galicia (Spain), Energy 82 (2015) 138–146.

[26] N. Arean, R. Carballo, G. Iglesias, An integrated approach for the installation of a wave farm, Energy 138 (2017) 910–919.

[27] A. Rute Bento, P. Martinho, C. Guedes Soares, Wave energy assessment for Northern Spain from a 33-year hindcast, Renewable Energy 127 (2018) 322–333.

[28] G. Lavidas, V. Venugopal, D. Friedrich, Wave energy extraction in Scotland through an improved nearshore wave atlas, International Journal of Marine Energy 17 (2017) 64–83.

[29] N. Guillou, G. Chapalain, Numerical modelling of nearshore wave energy resource in the Sea of Iroise, Renewable Energy 83 (2015) 942–953.

[30] N. Guillou, Evaluation of wave energy potential in the Sea of Iroise with two spectral models, Ocean Engineering 106 (2015) 141–151.

[31] R. Henderson, Design, simulation, and testing of a novel hydraulic power take-off system for the Pelamis wave energy converter, Renewable Energy 31 (2006) 271–283.

[32] A. Weinstein, G. Fredrikson, M. Park, K. Nielsen, Aqua Buoy - The offshore wave energy converter: Numerical modeling and optimization, in: Proceedings of Oceans '04 MTS/IEEE Techno-Ocean '04, Kobe, Japan, 2004.

[33] J. Kofoed, P. Frigaard, E. Friis-Madsen, H. Sørensen, Prototype testing of the wave energy converter Wave Dragon, Renewable Energy 31 (2006) 181–189.

[34] SHOM, Courants de marée - Mer d'Iroise de l'île Vierge à la pointe de Penmarc'h, Technical Report 560-UJA, Service Hydrographique et Océanographique de la Marine, 2016.

[35] N. Guillou, G. Chapalain, Tidal Turbines' Layout in a Stream with Asymmetry and Misalignment, Energies 10 (11) (2017) 1892.

[36] N. Guillou, S. P. Neill, P. E. Robins, Characterising the tidal stream power resource around France using a high-resolution harmonic database, Renewable Energy 123 (2018) 706–718.

[37] N. Guillou, G. Chapalain, E. Duvieilbourg, Modelling impact of bottom roughness on sea surface temperature in the Sea of Iroise, Continental Shelf Research 54 (2013) 80–92.

[38] N. Guillou, G. Chapalain, S. P. Neill, The influence of waves on the tidal kinetic energy resource at a tidal stream energy site, Applied Energy 180 (2016) 402–415.

[39] N. Guillou, Modelling effects of tidal currents on waves at a tidal stream energy site, Renewable Energy 114 (2017) 180–190.

[40] E. Boudière, C. Maisondieu, F. Ardhuin, M. Accensi, L. Pineau-Guillou, J. Lepesqueur, A suitable metocean hindcast database for the design of marine energy converters, International Journal of Marine Energy 3-4 (2013) 40–52.

[41] M. Gonçalves, P. Martinho, C. Soares, Wave energy conditions in the western French coast, Renewable Energy 62 (2014) 155–163.

[42] P. Gleizon, F. Campuzano, P. Carracedo, A. Martinez, J. Goggins, R. Atan, S. Nash, Wave Energy Resources Along the European Atlantic Coast, in: Z. Yang, A. Copping (Eds.), Marine Renewable Energy, Cherbourg, France, 2017.

[43] Conseil Départemental du Finistère, Atlas de l'environnement - édition 2017, Tech. Rep., Finistère - Penn-ar-Bed, 2017.

[44] N. Booij, R. Ris, L. Holthuijsen, A third-generation wave model for coastal regions, 1. Model description and validation, Journal of Geophysical Research 104 (C4) (1999) 7649–7666.

[45] T. Davey, V. Venugopal, H. Smith, G. Smith, J. Lawrence, L. Cavaleri, L. Bertotti, M. Prevostot, F. Girard, B. Holmes, Protocols for wave and tidal resource assessment - Equitable Testing and Evaluation of Marine Energy Extraction Devices in terms of Performances (EquiMar), Technical Report, Commission of the European Communities, 2010.

[46] G. Iglesias, R. Carballo, Wave energy potential along the Death Coast (Spain), Energy 34 (2009) 1963–1975.

[47] R. Carballo, M. Sánchez, V. Ramos, F. Taveira-Pinto, G. Iglesias, A high resolution geospatial database for wave energy exploitation, Energy 68 (2014) 542–583.

[48] D. Silva, A. Rute Bento, P. Martinho, C. Guedes Soares, High resolution local wave modelling in

the Iberian Peninsula, Energy 91 (2015) 1099–1112.

[49] P. Bénard, ALADIN-NH/AROME dynamical core; status and possible extension to IFS, in: Proceedings of the ECMWF Seminar, 714–726, 2004.

[50] J. M. Hervouet, Hydrodynamics of free surface flows, modelling with the finite element method, Cambridge University Press, Cambridge, 2007.

[51] F. Ardhuin, M. Accensi, IOWAGA - WW3 - HINDCAST - North East Atlantic grid - CFSR, https://sextant.ifremer.fr/record/f7458830-9357-4b81-8181-5492544d0a97/, 2013.

[52] A. Wacher, K. Nielsen, Mathematical and Numerical Modeling of the AquaBuOY Wave Energy Converter, Mathematics-in-Industry Case Studies Journal 2 (2010) 16–33.

[53] M. Veigas, M. López, P. Romilla, R. Carballo, A. Castor, G. Iglesias, A proposed wave farm on the Galician coast, Energy Conversion and Management 99 (2015) 102–111.

[54] A. Cornett, A global wave energy resource assessment, in: Proceedings of the International Journal of Offshore and Polar Engineering, 2008.

[55] J. Pastor, Y. Liu, Wave Climate Resource Analysis Based on a Revised Gamma Spectrum for Wave Energy Conversion Technology, Sustainability 8 (1321).

[56] Pelamis, Pelamis, P-750 wave energy converter, http://ctp.lns.mit.edu/energy/files/pelamisbrochure.pdf, 2018.

[57] SHOM, MNT Bathymétrique de la façade Atlantique (Projet HOMONIM), Documentation available at http://diffusion.shom.fr/produits/bathymetrie/mnt-facade-atl-homonim.html, 2017.

[58] Commissariat Général au Développement Durable, Chiffres et Statistiques - Consommations énergétiques des ménages en 2012, Technical Report 645, Commissariat Général au Développement Durable, 2015.

[59] G. Mattarolo, F. Lafon, M. Benoit, Wave energy resource of the French coasts: the ANEMOC database applied to the energy yield evaluation of wave energy converters, in: Proceedings of the 8th European Wave and Tidal Energy Conference, Uppsala, Sweden, 2009.

[60] N. Guillou, Wave energy dissipation by bottom friction in the English Channel, Ocean Engineering 82 (2014) 42–51.

[61] S. Neill, M. Hashemi, Wave power variability over the northwest European shelf seas, Applied Energy 106 (2013) 31–46.